



HAL
open science

Optimization of a dedicated protocol using a small-voxel PSF reconstruction for head-and-neck 18FDG PET/CT imaging in differentiated thyroid cancer

Renaud Ciappuccini, Cédric Desmots, Idir Licaj, Cécile Blanc-Fournier, Stéphane Bardet, Nicolas Aide

► To cite this version:

Renaud Ciappuccini, Cédric Desmots, Idir Licaj, Cécile Blanc-Fournier, Stéphane Bardet, et al.. Optimization of a dedicated protocol using a small-voxel PSF reconstruction for head-and-neck 18FDG PET/CT imaging in differentiated thyroid cancer. *EJNMMI Research*, 2018, 8 (1), pp.104. 10.1186/s13550-018-0461-x . inserm-02106944

HAL Id: inserm-02106944

<https://inserm.hal.science/inserm-02106944>

Submitted on 23 Apr 2019

HAL is a multi-disciplinary open access archive for the deposit and dissemination of scientific research documents, whether they are published or not. The documents may come from teaching and research institutions in France or abroad, or from public or private research centers.

L'archive ouverte pluridisciplinaire **HAL**, est destinée au dépôt et à la diffusion de documents scientifiques de niveau recherche, publiés ou non, émanant des établissements d'enseignement et de recherche français ou étrangers, des laboratoires publics ou privés.

ORIGINAL RESEARCH

Open Access



Optimization of a dedicated protocol using a small-voxel PSF reconstruction for head-and-neck ^{18}F FDG PET/CT imaging in differentiated thyroid cancer

Renaud Ciappuccini^{1,2*} , Cédric Desmots³, Idir Licaj⁴, Cécile Blanc-Fournier⁵, Stéphane Bardet¹ and Nicolas Aide^{2,3}

Abstract

Background: ^{18}F FDG PET/CT is crucial before neck surgery for nodal recurrence localization in iodine-refractory differentiated or poorly differentiated thyroid cancer (DTC/PDTC). A dedicated head-and-neck (HN) acquisition performed with a thin matrix and point-spread-function (PSF) modelling in addition to the whole-body PET study has been shown to improve the detection of small cancer deposits. Different protocols have been reported with various acquisition times of HN PET/CT. We aimed to compare two reconstruction algorithms for disease detection and to determine the optimal acquisition time per bed position using the Siemens Biograph6 with extended field-of-view.

Methods: Twenty-one consecutive and unselected patients with DTC/PDTC underwent HN PET/CT acquisition using list-mode. PET data were reconstructed, mimicking five different acquisition times per bed position from 2 to 10 min. Each PET data set was reconstructed using 3D-ordered subset expectation maximisation (3D-OSEM) or iterative reconstruction with PSF modelling with no post filtering ($\text{PSF}_{\text{allpass}}$). These reconstructions resulted in 210 anonymized datasets that were randomly reviewed to assess ^{18}F FDG uptake in cervical lymph nodes or in the thyroid bed using a 5-point scale. Noise level, maximal standard uptake values (SUV_{max}), tumour/background ratios (TBRs) and dimensions of the corresponding lesion on the CT scan were recorded. In surgical patients, the largest tumoral size of each lymph node metastasis was measured by a pathologist.

Results: The 120 HN PET studies of the 12 patients with at least 1 ^{18}F FDG focus scored malignant formed the study group. Noise level significantly decreased between 2 and 4 min for both 3D-OSEM and $\text{PSF}_{\text{allpass}}$ reconstructions ($p < 0.01$). TBRs were similar for all the acquisition times for both 3D-OSEM and $\text{PSF}_{\text{allpass}}$ reconstructions ($p = 0.25$ and 0.44 , respectively). The detection rate of malignant foci significantly improved from 2 to 10 min for $\text{PSF}_{\text{allpass}}$ reconstruction (20/26 to 26/26; $p = 0.01$) but not for 3D-OSEM (15/26 to 19/26; $p = 0.26$). For each of the five acquisition times, $\text{PSF}_{\text{allpass}}$ detected more malignant foci than 3D-OSEM ($p < 0.01$). In the seven surgical patients, $\text{PSF}_{\text{allpass}}$ evidenced smaller malignant lymph nodes than 3D-OSEM at 8 and 10 min. At 10 min, the mean size of the lymph node metastases neither detected with $\text{PSF}_{\text{allpass}}$ nor 3D-OSEM was 3 ± 0.6 mm vs 5.8 ± 1.1 mm for those detected with $\text{PSF}_{\text{allpass}}$ only and 10.9 ± 3.3 for those detected with both reconstructions ($p < 0.001$).

Conclusions: $\text{PSF}_{\text{allpass}}$ HN PET improves lesion detectability as compared with 3D-OSEM HN PET. $\text{PSF}_{\text{allpass}}$ with an acquisition time between 8 and 10 min provides the best performance for tumour detection.

Keywords: ^{18}F FDG PET/CT, List-mode acquisition, Point spread function, Head and neck imaging, Thyroid cancer

* Correspondence: r.ciappuccini@baclesse.unicancer.fr

¹Department of Nuclear Medicine and Thyroid Unit, François Baclesse Cancer Centre, 3 Avenue Général Harris, 14000 Caen, France

²INSERM 1086 ANTICIPE, Normandie University, Caen, France

Full list of author information is available at the end of the article

Background

^{18}F FDG PET/CT is crucial before neck surgery for nodal recurrence detection in radioiodine-refractory differentiated or poorly differentiated thyroid cancer (DTC/PDTC), as the surgeon's plan is mainly guided by PET/CT and neck US data. In this setting, a dedicated head-and-neck PET/CT acquisition (HN PET) performed with a thin matrix and point-spread-function (PSF) modelling in addition to the whole-body (WB) PET study has been shown to improve the detection of small cancer deposits [1]. Various HN PET/CT protocols have been reported for head-and-neck malignancies including thyroid cancers, with different algorithm reconstructions (mainly without PSF) and with different acquisition times ranging from 6 to 15 min [1–5]. In this context, to manage patients' schedules of a busy PET unit, it would be helpful to optimise the acquisition time of such a complementary HN PET acquisition for routine practice. The goal would be to determine the acquisition time that allows high sensitivity for disease detection, without uselessly increasing the whole PET acquisition time. Furthermore, PSF and ordered subset expectation maximisation (OSEM) reconstructions have not been compared for head-and-neck (HN) imaging with various acquisition times. We aimed to compare these two reconstruction algorithms for the detection of thyroid cancer recurrence in the neck and to determine the optimal acquisition time per bed position using the Siemens Biograph6 with extended field-of-view.

Methods

Patient selection

Twenty-one consecutive and unselected patients with DTC/PDTC who underwent an ^{18}F FDG PET/CT scan with a complementary dedicated HN PET/CT acquisition between June 2015 and November 2017 in our department were reviewed. All had a negative post-therapeutic ^{131}I WB scan.

PET/CT

PET/CT acquisitions were performed using a PET/CT scanner (Biograph TrueV, Siemens Medical Solutions) with a six-slice spiral CT component and an extended field-of-view of 21.6 cm. Patients were asked to fast for ≥ 6 h before ^{18}F FDG injection (4.0 ± 0.2 MBq per kg). Blood glucose level was 6.0 ± 1.7 mmol/l. WB PET/CT images were performed 58 ± 3 min post injection from mid-thigh to the base of the skull with an acquisition time per bed position of 2 min and 40 s in patients of low and average weight (i.e. body mass index [BMI] < 25 kg/m 2) or 3 min and 40 s in overweight patients (i.e. BMI ≥ 25 kg/m 2). HN PET was performed either immediately after the WB acquisition and patient repositioning (3 ± 2 min between WB and HN PET, 14

patients) or after the WB acquisition of the next-scheduled patient (18 ± 5 min between WB and HN PET, 7 patients). HN PET/CT data sets were acquired in list-mode (LM) using a single-bed position of 10 min from the base of the skull to the superior mediastinum. All patients were repositioned with arms along the chest. A low-dose CT scan was acquired prior to HN PET/CT with the same longitudinal field of view. CT parameters were set to 100 mAs and 130 kV, slice thickness of 2.5 mm and pitch 1.

Image reconstruction

PET raw data were reconstructed with the PSF reconstruction algorithm (HD; TrueX, Siemens Medical Solutions; 3 iterations and 21 subsets) without filtering (PSF_{allpass}) [6] and with the 3D-OSEM reconstruction algorithm (4 iterations and 8 subsets). Scatter and attenuation corrections were carried out. For all HN PET reconstructions, matrix size was 256×256 (vs. 168×168 for WB acquisition), resulting in a $2.67 \times 2.67 \times 2.67$ mm voxel size (small-voxels). For each PSF_{allpass} or 3D-OSEM reconstruction, five datasets were reconstructed from this LM acquisition, from 2 to 10 min with a 2-min increment. Overall, ten HN PET data sets were obtained per patient.

^{18}F FDG-PET/CT scan interpretation

All images were blindly reviewed after randomisation by an experienced nuclear medicine physician on a digital workstation (eSoft/TrueD workstation, Siemens Medical Solutions). The randomisation was performed as follows: all data sets of 2 min were first randomly pooled together, and then those of 4, 6, 8 and 10 min. Overall, 210 anonymized PET data sets were reviewed during separate reading sessions (8 weeks apart).

The reader reported each ^{18}F FDG focus on HN PET images and graded its uptake on a scale of 1–5 (1, definitely benign; 2, probably benign; 3, indeterminate; 4, probably malignant; and 5, definitely malignant). Maximum standardised uptake value (SUV_{max}) was measured according to EANM guidelines [7]. Mean standardised uptake value (SUV_{mean}) of the vascular background was measured in the large neck vessels (carotid artery and internal jugular vein). The noise was calculated as follows:
$$\frac{\text{standard derivation of SUV in the vascular background}}{\text{SUV}_{\text{mean in the vascular background}}} \times 100$$
. The tumour/background ratio (TBR) of an ^{18}F FDG focus was computed as follows:
$$\frac{\text{SUV}_{\text{max in the lymph node or the local tumour}}}{\text{SUV}_{\text{mean in the vascular background}}}$$

Lymph nodes or thyroid bed lesions corresponding to ^{18}F FDG foci identified on co-registered CT images were also reported.

At the patient level, the HN PET/CT study was scored either negative (^{18}F FDG foci all scored 1 or 2), indeterminate

(no ¹⁸FDG focus scored higher than 3), or positive (≥ 1 ¹⁸FDG focus scored 4 or 5).

Surgery and follow-up were the reference standard for ¹⁸FDG foci at head-and-neck level.

Pathology was the gold standard in surgical patients. The largest tumoral size of each lymph node metastasis was estimated by one pathologist.

Statistical analysis

Quantitative data are expressed in mean ± standard deviation (SD), or median (min-max). The nonparametric Mann-Whitney *U* test for paired samples was used to compare noise levels, TBRs, and SUVmax at different time points. For all tests, a two-tailed *p* value < 0.05 was considered statistically significant. Graphs and statistics were performed using Prism (GraphPad software, La Jolla, CA) and Vassar University clinical research calculators (<http://vassarstats.net/>).

Results

Patients' characteristics

Of the 21 DTC/PDTC patients, 16 had neck US abnormalities and/or biochemical disease (elevated serum thyroglobulin [Tg] levels or rising anti-Tg antibodies [TgAb] levels), three had metastatic disease under surveillance and two were at high-risk [8] before first radioiodine administration.

Twelve out of 21 patients had at least 1 ¹⁸FDG uptake suggestive of a tumour (i.e. score ≥ 4) on HN PET. All the 26 ¹⁸FDG findings of score ≥ 4 in these 12 patients were confirmed as truly malignant after surgery (*n* = 7) or follow-up on PET/CT (*n* = 5).

Of the nine patients with a negative PET/CT, five had a persistent biological disease without persistent/recurrent

disease (PRD) during follow-up, two had ¹⁸FDG-negative lymph node involvement with positive US (pathological confirmation after surgery), one had a ¹⁸FDG true-negative study with false-positive lymph node involvement on US (confirmed as benign after surgery) and one had a subsequent ¹⁸FDG-positive PET/CT study after biological disease progression during follow-up.

Noise level

For both 3D-OSEM and PSF_{allpass} reconstructions, the noise significantly decreased between 2 and 4 min (*p* = 0.007). Also, the noise significantly decreased for PSF_{allpass} reconstruction between 2 and 10 min (*p* = 0.016), and between 4 and 10 min (*p* = 0.042) (Fig. 1a, b).

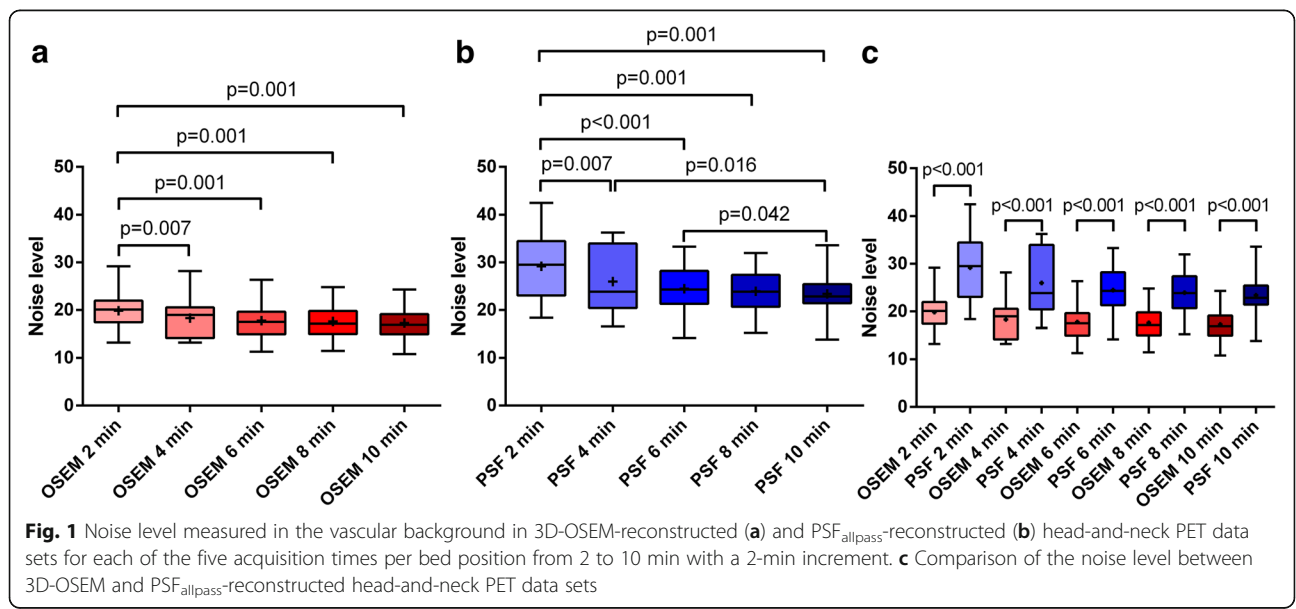
The noise was significantly higher with PSF_{allpass} than 3D-OSEM reconstruction for each of the five acquisition times per bed position from 2 to 10 min (Fig. 1c).

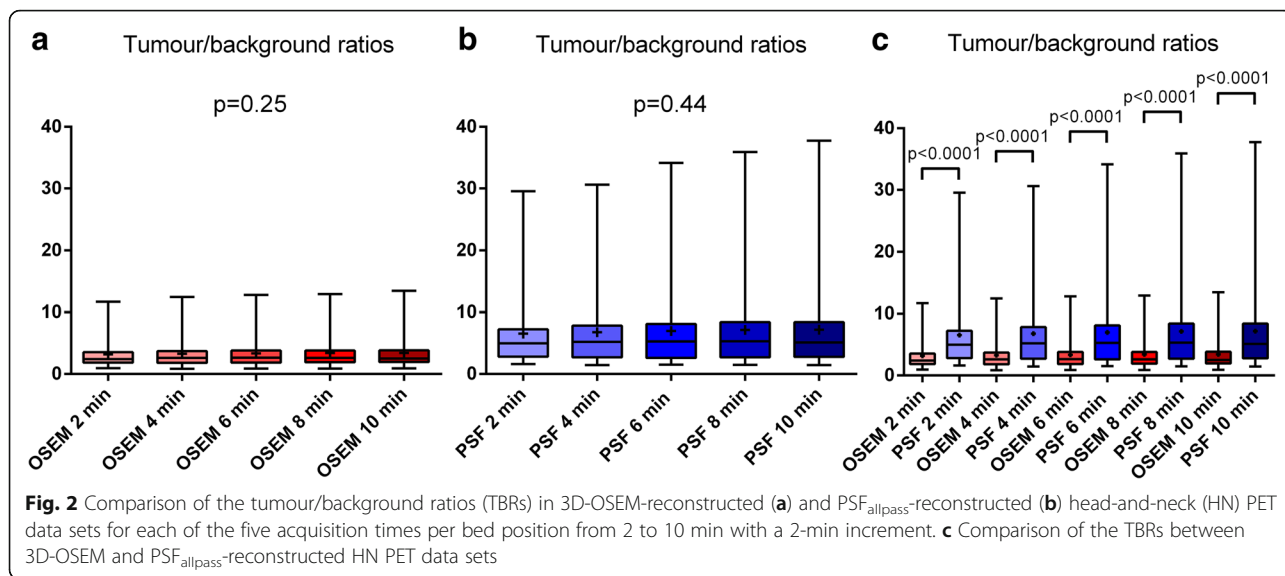
Tumour/background ratios

For 3D-OSEM reconstruction, TBRs were similar for all acquisition times per bed position (*p* = 0.25). The same results were observed for PSF_{allpass} reconstruction (*p* = 0.44) (Fig. 2a, b). TBRs were higher with PSF_{allpass} than with 3D-OSEM reconstruction for each of the five acquisition times per bed position (Fig. 2c).

For both 3D-OSEM and PSF_{allpass} reconstructions, TBRs were significantly higher in detectable lesions than in undetectable lesions for each of the five acquisition times per bed position (Fig. 3).

For each acquisition time and for each reconstruction, the SUVmax of the lesions not detected were not statistically different from the SUVmax measured in the vascular background (Fig. 4).





Lesion detectability

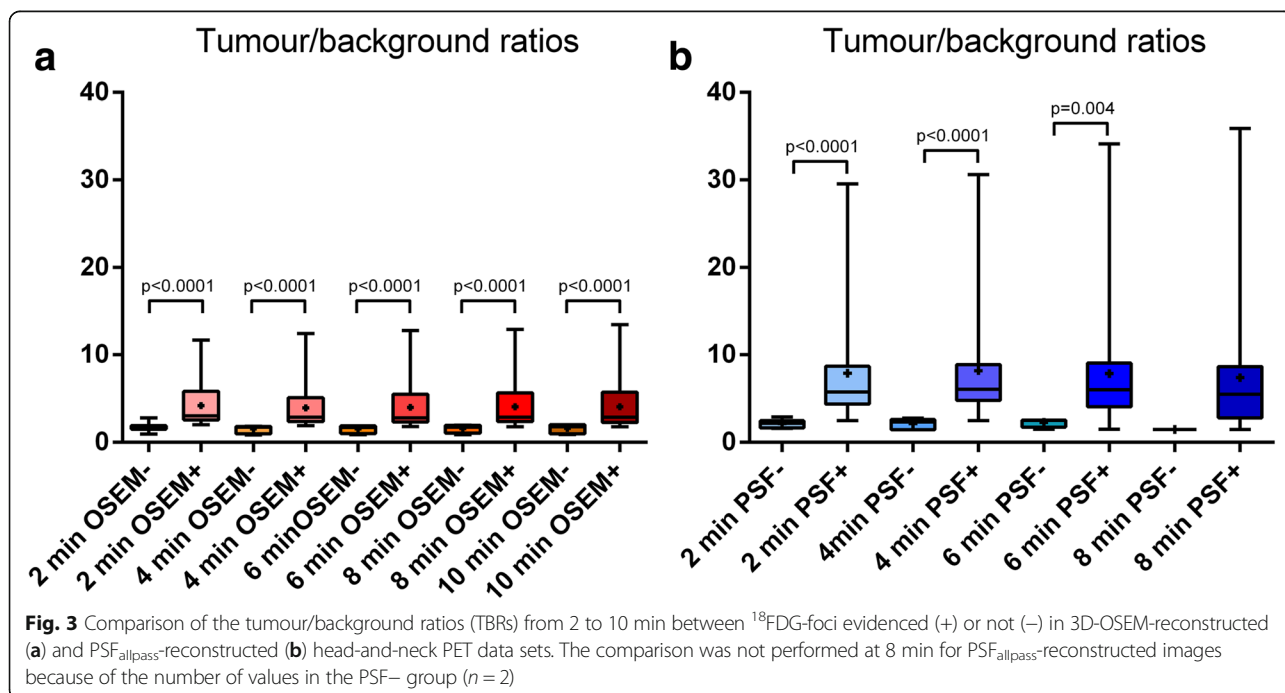
For each acquisition time from 2 to 10 min, 3D-OSEM reconstruction detected 15, 19, 19, 19 and 19 lesions, respectively ($p = 0.26$), while PSF_{allpass} reconstruction detected 20, 20, 22, 25 and 26 lesions, respectively ($p = 0.01$). Figures 5 and 6 present examples of mismatches between 3D-OSEM and PSF_{allpass} HN PET data sets reading.

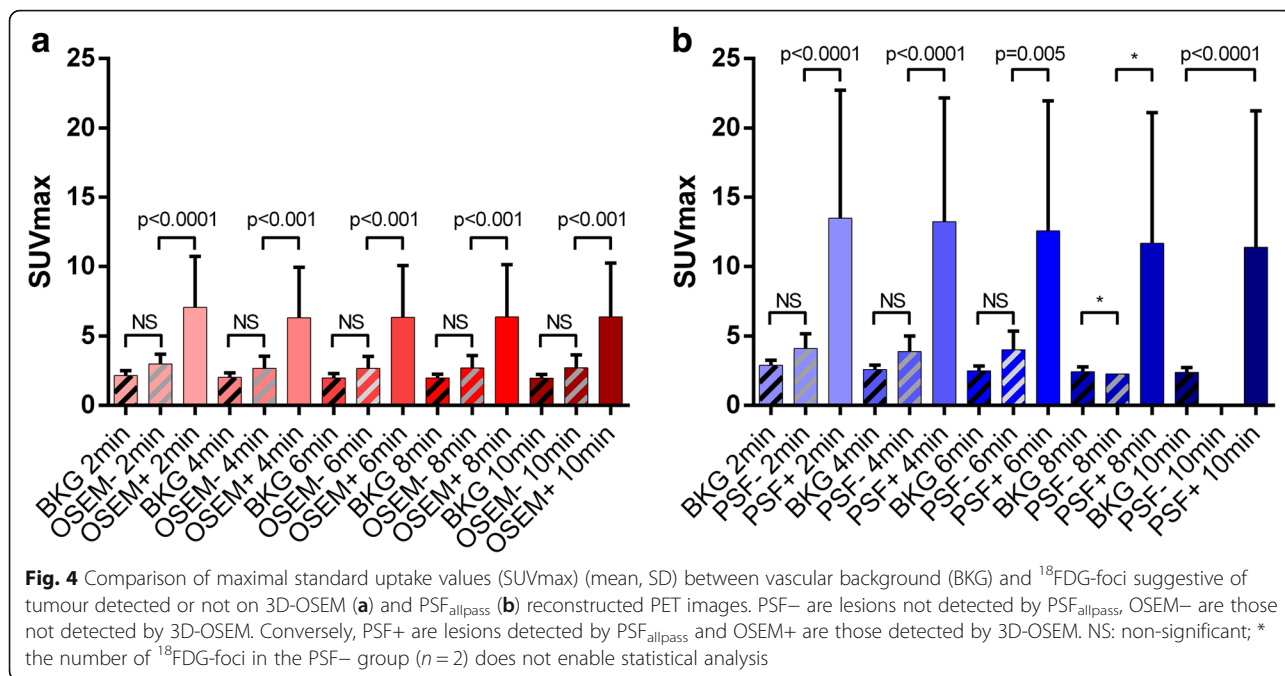
When comparing both reconstructions at each of the five acquisition times per bed position from 2 to 10 min, PSF_{allpass} performed better than 3D-OSEM for lesion detection ($p < 0.01$, $p < 0.0001$, $p < 0.01$, $p = 0.02$ and $p < 0.01$, respectively).

In the seven surgical patients, PSF_{allpass} detected smaller malignant lymph nodes than 3D-OSEM at 8 and 10 min (Fig. 7). At 10 min, the mean size of the lymph node metastases neither detected with PSF_{allpass} nor 3D-OSEM was 3 ± 0.6 mm vs 5.8 ± 1.1 mm for those detected with PSF_{allpass} only and 10.9 ± 3.3 mm for those detected with both reconstructions ($p < 0.001$).

Discussion

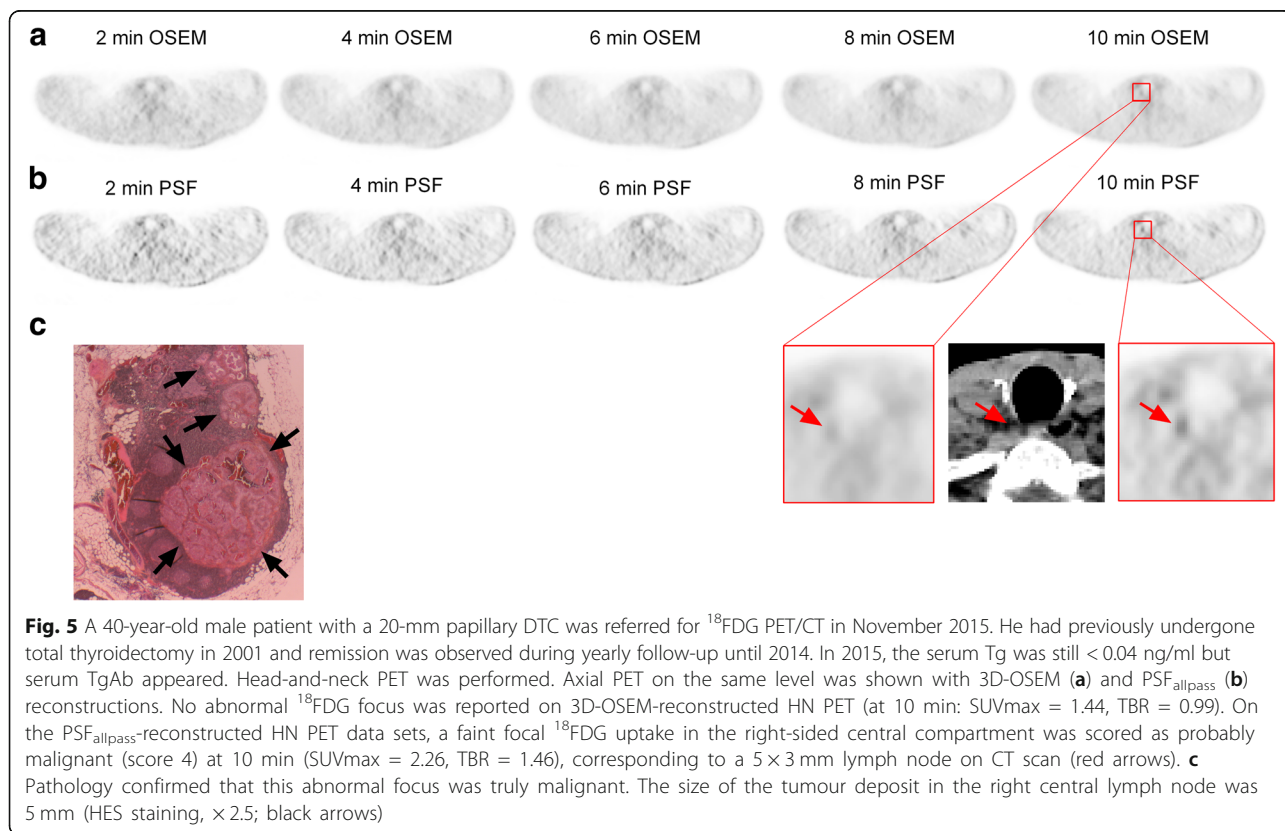
To date, several PET/CT studies have explored recurrent disease in the neck for thyroid malignancies with various protocols using WB or HN PET, different acquisition times,





reconstruction algorithms or delayed images. The results of these studies are difficult to compare to each other. To our knowledge, no study has previously determined the optimal acquisition time using PSF reconstruction. We observed that 4 min was the minimal acquisition time for both

PSF_{allpass} and 3D-OSEM HN PET to overcome the noise level. We further showed that an increase of the PSF_{allpass} acquisition time to either 8 or 10 min provided the best performance for lymph node or local recurrence diagnosis in DTC/PDTC.



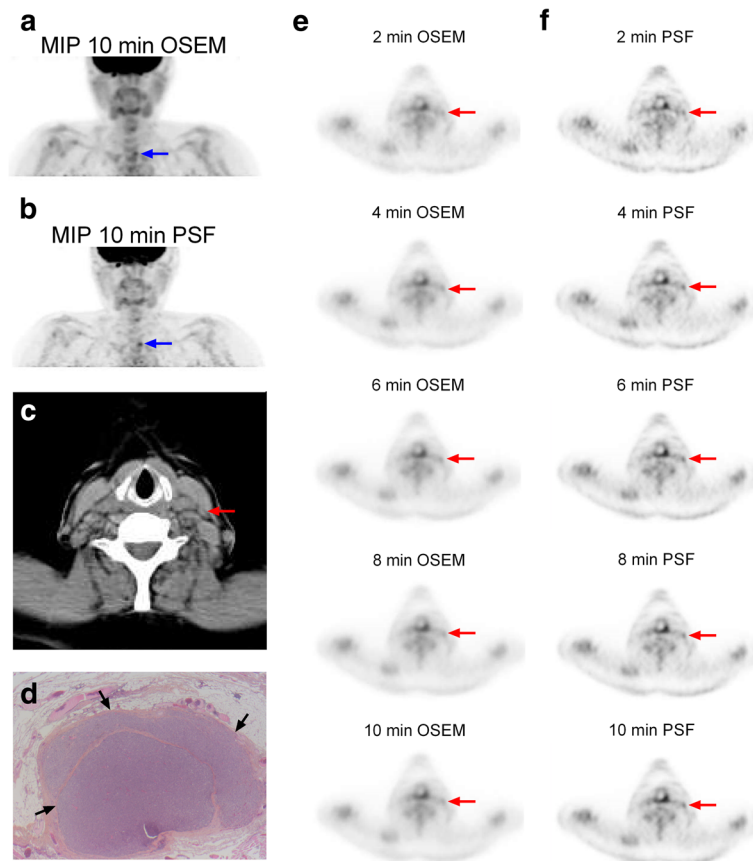
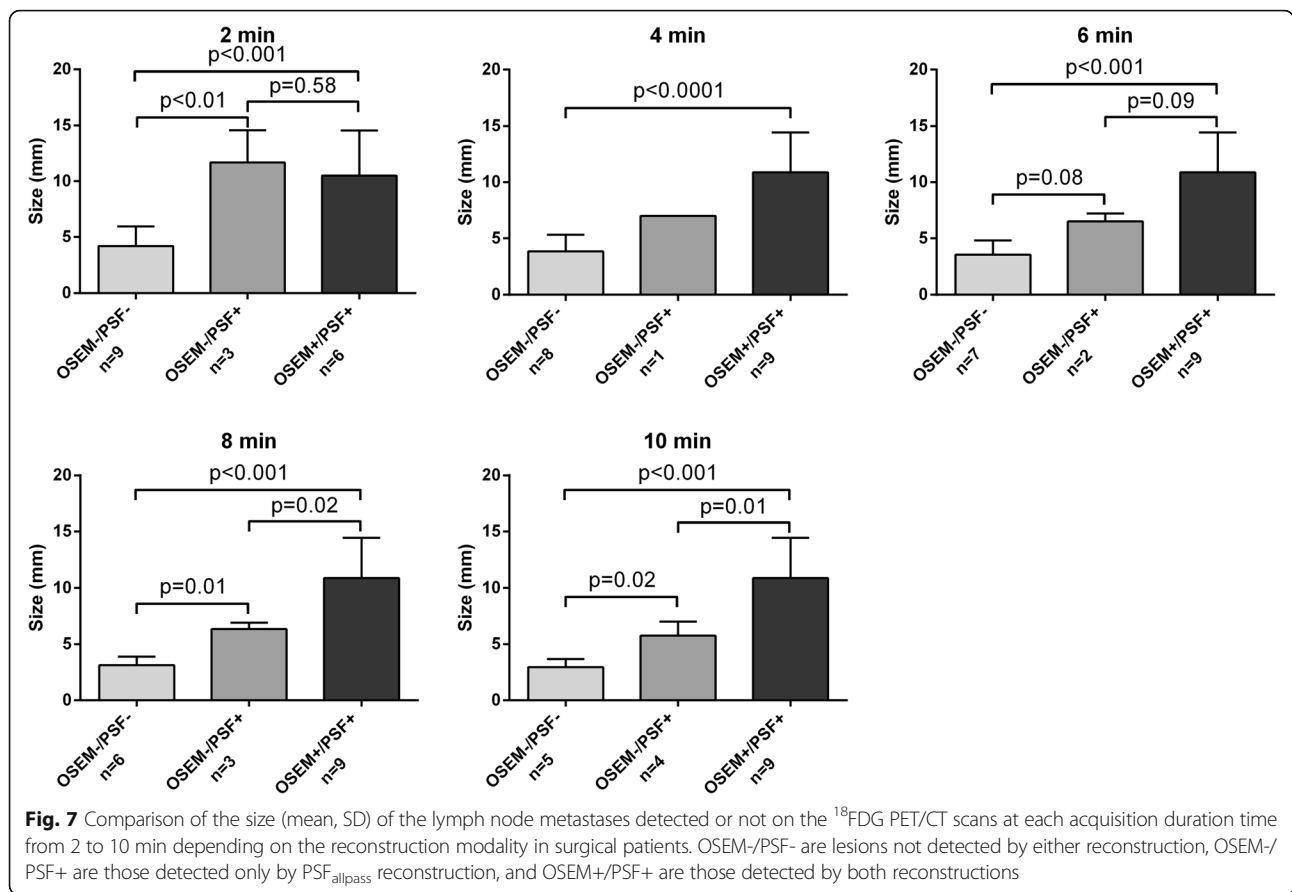


Fig. 6 A 62-year-old female patient with a 70-mm PDTC (pT3 Nx Mx) was referred for ^{18}F FDG PET/CT in November 2017 to explore a detectable serum Tg level under levothyroxine (11 ng/ml, without serum TgAb) 2 years after initial ^{131}I treatment. Maximum intensity projection images (MIP) showed lymph node involvement of the left central compartment on both 3D-OSEM-reconstructed HN PET (**a**, blue arrow) and $\text{PSF}_{\text{allpass}}$ -reconstructed HN PET (**b**, blue arrow). No abnormal ^{18}F FDG focus (score ≤ 3) was reported on 3D-OSEM-reconstructed HN PET in the left lateral compartment (at 10 min: SUVmax = 1.67, TBR = 1.19) (**e**). On the $\text{PSF}_{\text{allpass}}$ -reconstructed HN PET data sets (**f**), a small focal ^{18}F FDG uptake in the left lateral compartment was scored as probably malignant (score 4) at 4–10 min (at 10 min: SUVmax = 2.43, TBR = 1.74), corresponding to a 6 \times 4 mm lymph node on CT scan (**c**, red arrow). Left central and left lateral dissection was performed and confirmed lymph node involvement in both compartments. **d** The left lateral lymph node was massively invaded (black arrows). The size of the tumour deposit was 5 mm (HES staining, $\times 2.5$)

This study is the first to compare PSF modelling to conventional OSEM reconstruction with different acquisition times at the HN level. The protocol was designed for routine practical application. Indeed, adding a 10-min HN PET acquisition after the WB PET can be easily performed even in busy PET units. We have recently demonstrated that an HN PET acquisition offers a better diagnostic value than WB PET alone because of the following advantages: thinner matrix, longer acquisition time and reduced motion artefacts [1]. However, the previous studies for HN squamous cell cancers and thyroid malignancies reported a wide range of acquisition times for HN PET: 6 min [4], 8 min [1], 10 min [2], 12 min [5] or 15 min [3]. Thus, it seemed crucial to determine the time needed for an HN PET acquisition. In our study protocol, the longest acquisition for HN PET was 10 min because we felt that a dedicated acquisition

over 10 min was not suitable for routine practice to respect the patients' schedule and to fulfil good practice and EARL guidelines [7, 9]. Furthermore, our results can apply to both PET devices equipped or not with PSF reconstruction. PSF has been shown to increase the detection of small cancer lesions such as lymph node metastases in breast [10] and lung cancers [11]. Our data confirmed this finding for PRD in DTC/PDTC patients at the HN level.

We showed that although 3D-OSEM 4-min performances were close to those of $\text{PSF}_{\text{allpass}}$ at 4 min, a two-fold increase of the acquisition time with $\text{PSF}_{\text{allpass}}$ (i.e. 8 min) considerably increased ^{18}F FDG foci detection. Indeed, ^{18}F FDG foci detection continued to increase for $\text{PSF}_{\text{allpass}}$ after 4 min, whereas there was no significant added value in increasing the acquisition time for 3D-OSEM after 4 min. Detecting all malignant ^{18}F FDG



foci is of importance for the surgeon because the treatment plan (i.e. the number and the localization of the neck compartments to dissect) is affected by PET data. The limited number of surgical patients in the present study did not enable an investigation in which proportion the treatment plan was modified.

Several factors can account for better sensitivity with PSF_{allpass} than 3D-OSEM with time. First, the noise level significantly decreased between 2 and 4 min for both 3D-OSEM and PSF_{allpass}. Indeed, between 2 and 4 min, we observed a 26% increase in the lesion detection for 3D-OSEM. Second, small cancer lesions not evidenced on the CT scan alone because of their size can be evidenced on PET images if their SUV_{max} exceeded that measured in the vascular background. As previously reported [11], PSF reconstruction is expected to affect quantitative values in nodes <10 mm more than 3D-OSEM. We used the vascular background because neck PRD often occurs in lymph nodes that are close to the great vessels, such as in the lateral compartment. Interestingly, our results showed that detectability increased when SUV_{max} values of very small lesions (i.e. not identifiable on CT scans) were above the SUV_{max} measured in the background which may explain the increase of lesion detection with PSF.

We used one technical advantage of our PET device, which is an extended field-of-view, enabling to increase the detection sensitivity and explore the HN region with one bed position only. Then, time acquisition was reduced compared to PET devices which require two bed positions to image the same volume. Furthermore, the small-voxel matrix of our dedicated HN PET improves lymph node detection, as previously shown in the neck [1] and in the axillary region for breast cancer [12].

This study has some limitations. First, as previously pointed out [11], PSF and OSEM images can be identified as the latter appear smoother. This could be a potential bias in the case of a more sensitive interpretation of PSF images by the reader, as reported in other clinical studies [11]. Second, the study group involved a limited number of patients, as radioiodine-refractory recurrent DTC/PDTC is a rare condition. Third, 58% of the patients benefited from pathological confirmation, but careful follow-up in the remaining 42% of patients made us confident with the ¹⁸F-FDG malignancy status. Finally, the impact of time-of-flight (TOF) was not explored. Based on a phantom study, Rogasch et al. demonstrated higher spatial resolution for PSF + TOF than PSF alone [13] but the scan time was 3 min per bed position vs. 2 to 10 in our study. It is likely that for such dedicated

acquisitions with scan times of ≥ 4 min, as in our study, the lack of TOF has little impact.

Conclusions

PSF_{allpass} HN PET improves lesion detectability as compared with 3D-OSEM HN PET. PSF_{allpass} with an acquisition time between 8 and 10 min provides the best performance in the detection of tumour recurrence.

Acknowledgements

The authors thank Prof Pierre Rousselot, Department of Pathology, Centre Baclesse, Caen, France.

Funding

The authors received no specific funding for this work.

Availability of data and materials

The datasets used and analysed during the current study are available from the corresponding author on reasonable request.

Authors' contributions

RC and NA conceived the study and its design. RC performed data acquisition and drafted the manuscript. CD and CBF participated in the data acquisition. RC, IL, and NA performed the statistical analysis. NA, IL, and SB helped to draft the manuscript. All authors read and approved the final manuscript.

Ethics approval and consent to participate

The study procedures were in accordance with the ethical standards of the committees with responsibility for human experimentation and with the 1964 Helsinki Declaration and its later amendments. The local ethics committee waived informed consent for this type of study conducted in the setting of clinical indications (Ref A12-D24-VOL13, "Comité de protection des personnes Nord-Ouest III"). The patient records were anonymized prior to analysis.

Consent for publication

All patients gave written informed consent for publication.

Competing interests

The authors declare that they have no competing interests.

Publisher's Note

Springer Nature remains neutral with regard to jurisdictional claims in published maps and institutional affiliations.

Author details

¹Department of Nuclear Medicine and Thyroid Unit, François Baclesse Cancer Centre, 3 Avenue Général Harris, 14000 Caen, France. ²INSERM 1086 ANTICIPE, Normandie University, Caen, France. ³Department of Nuclear Medicine, University Hospital, Caen, France. ⁴Department of Clinical Research, François Baclesse Cancer Centre, Caen, France. ⁵Department of Pathology, François Baclesse Cancer Centre, Caen, France.

Received: 14 September 2018 Accepted: 21 November 2018

Published online: 03 December 2018

References

- Ciappuccini R, Aide N, Blanchard D, Rame JP, de RD MJJ, et al. Incremental value of a dedicated head and neck acquisition during 18F-FDG PET/CT in patients with differentiated thyroid Cancer. *PLoS One*. 2016;11:e0162482.
- Chatziioannou SN, Georgakopoulos AT, Pianou NK, Kafiri GT, Pavlou SN, Kallergi M. Recurrent thyroid cancer diagnosis: ROC study of the effect of a high-resolution head and neck 18F-FDG PET/CT scan. *Acad Radiol*. 2014;21:58–63.
- Davison JM, Stocker DJ, Montilla-Soler JL, Jurgens JS, Allen TW, Holley TS, et al. The added benefit of a dedicated neck F-18 FDG PET-CT imaging

protocol in patients with suspected recurrent differentiated thyroid carcinoma. *Clin Nucl Med*. 2008;33:464–8.

- Kunawudhi A, Pak-art R, Keelawat S, Tepmongkol S. Detection of subcentimeter metastatic cervical lymph node by 18F-FDG PET/CT in patients with well-differentiated thyroid carcinoma and high serum thyroglobulin but negative 131I whole-body scan. *Clin Nucl Med*. 2012;37:561–7.
- Rodrigues RS, Bozza FA, Christian PE, Hoffman JM, Butterfield RI, Christensen CR, et al. Comparison of whole-body PET/CT, dedicated high-resolution head and neck PET/CT, and contrast-enhanced CT in preoperative staging of clinically M0 squamous cell carcinoma of the head and neck. *J Nucl Med*. 2009;50:1205–13.
- Kadmas DJ, Casey ME, Conti M, Jakoby BW, Lois C, Townsend DW. Impact of time-of-flight on PET tumor detection. *J Nucl Med*. 2009;50:1315–23.
- Boellaard R, Delgado-Bolton R, Oyen WJ, Giammarile F, Tatsch K, Eschner W, et al. FDG PET/CT: EANM procedure guidelines for tumour imaging: version 2.0. *Eur J Nucl Med Mol Imaging*. 2015;42:328–54.
- Haugen BR, Alexander EK, Bible KC, Doherty GM, Mandel SJ, Nikiforov YE, et al. 2015 American Thyroid Association management guidelines for adult patients with thyroid nodules and differentiated thyroid Cancer: the American Thyroid Association guidelines task force on thyroid nodules and differentiated thyroid Cancer. *Thyroid*. 2016;26:1–133.
- Boellaard R, O'Doherty MJ, Weber WA, Mottaghy FM, Lonsdale MN, Stroobants SG, et al. FDG PET and PET/CT: EANM procedure guidelines for tumour PET imaging: version 1.0. *Eur J Nucl Med Mol Imaging*. 2010;37:181–200.
- Bellefleur D, Blanc FC, Switsers O, Dugue AE, Levy C, Allouache D, et al. Staging the axilla in breast cancer patients with (1)(8)F-FDG PET: how small are the metastases that we can detect with new generation clinical PET systems? *Eur J Nucl Med Mol Imaging*. 2014;41:1103–12.
- Lasnon C, Hicks RJ, Beaugerard JM, Milner A, Paciencia M, Guizard AV, et al. Impact of point spread function reconstruction on thoracic lymph node staging with 18F-FDG PET/CT in non-small cell lung cancer. *Clin Nucl Med*. 2012;37:971–6.
- Koopman D, van Dalen JA, Arkies H, Oostdijk AHJ, Francken AB, Bart J, et al. Diagnostic implications of a small-voxel reconstruction for loco-regional lymph node characterization in breast cancer patients using FDG-PET/CT. *EJNMMI Res*. 2018;8:3.
- Rogasch JM, Hofheinz F, Lougovski A, Furth C, Ruf J, Grosser OS, et al. The influence of different signal-to-background ratios on spatial resolution and F18-FDG-PET quantification using point spread function and time-of-flight reconstruction. *EJNMMI Phys*. 2014;1:12.

Submit your manuscript to a SpringerOpen[®] journal and benefit from:

- Convenient online submission
- Rigorous peer review
- Open access: articles freely available online
- High visibility within the field
- Retaining the copyright to your article

Submit your next manuscript at ► springeropen.com